

A practical method for gas changing time estimation using a simple gas-liquid mass transfer model

Original

A practical method for gas changing time estimation using a simple gas-liquid mass transfer model / Tarraran, L.; Lueckel, F. B.; Tommasi, T.; Contador, F. I. S.; Fino, D.. - In: JOURNAL OF MICROBIOLOGICAL METHODS. - ISSN 0167-7012. - 200:(2022). [10.1016/j.mimet.2022.106544]

Availability:

This version is available at: 11583/2981636 since: 2023-09-05T09:14:15Z

Publisher:

ELSEVIER

Published

DOI:10.1016/j.mimet.2022.106544

Terms of use:

This article is made available under terms and conditions as specified in the corresponding bibliographic description in the repository

Publisher copyright

Elsevier postprint/Author's Accepted Manuscript

© 2022. This manuscript version is made available under the CC-BY-NC-ND 4.0 license
<http://creativecommons.org/licenses/by-nc-nd/4.0/>. The final authenticated version is available online at:
<http://dx.doi.org/10.1016/j.mimet.2022.106544>

(Article begins on next page)

A Practical Method for Gas Changing Time Estimation Using a Simple Gas-Liquid Mass Transfer Model

Loredana Tarraran ^{a*}, Fabio Bozzolo Lueckel ^{b*}, Tonia Tommasi ^a, Felipe Ignacio Scott Contador ^c, Debora Fino ^a

^a Department of Applied Science and Technology, Politecnico di Torino, Corso Duca degli Abruzzi 24, Torino, 10129, Italy.

^b Escuela de Ingeniería Bioquímica, Pontificia Universidad Católica de Valparaíso, Avenida Brasil 2147, Valparaíso, Chile.

^c Green Technology Research Group, Facultad de Ingeniería y Ciencias Aplicadas, Universidad de los Andes, Monseñor Álvaro del Portillo 12455, Santiago, Chile.

* These authors equally contributed to this work.

Formatted: Not Highlight

Abstract

The present work explains a practical and simple method to calculate the gas changing time of anaerobic systems. It is substantiated under the physics of gas-liquid transfer theory and allows researchers to obtain an approximate value of gas changing time with few measurements of the gas composition in the outlet of the reactor. The only analytical equipment required is a gas analyzer, and calculations can be done using a spreadsheet. Along with the validation of the model, a short guide for its application in the laboratory is introduced. The model fit the experimental data with less than 1% error in the composition of the out-gas when no carbon dioxide is involved. This method will allow savings in

24 valuable resources such as time and gases while providing greater comprehension of the
25 characteristics of the gas-liquid transfer of the studied system.

26 **Keywords**

27 Anaerobic fermentation; gas changing time; oxygen purging.

28 **1. Introduction**

29 Nowadays, the industry and research on bulk chemicals and third-generation biofuels based
30 on carbon gases are growing because of the rising sensibility and higher regulations about
31 decreasing greenhouse gas emissions. In particular, one of the more attractive carbon
32 feedstocks is CO₂ due to its large availability and contribution to climate change. Several
33 different agents, such as chemical catalysts, enzymes, and microorganisms can convert it into
34 added-value compounds of industrial interest (Chauvy et al., 2019; Saravanan et al., 2021;
35 Shi et al., 2015). According to the catalyst's nature, many CO₂ valorization processes occur
36 in a liquid phase (usually water). The constant development of these technologies led to the
37 establishment of different technologies to measure a specific gas (especially O₂ and CO₂) in
38 the liquid phase.

39 In the case of CO₂ valorization employing anaerobic bacteria, the lack of oxygen and supply
40 of feedstock is required. Nevertheless, these needs are often performed in two steps before
41 inoculation for technical, environmental, and economic reasons. The first step is sparging the
42 liquid phase with nitrogen to purge oxygen, and then the second is providing the gaseous
43 feedstock.

44 In the literature, many protocols used nowadays involve a preparation step before starting the
45 fermentation with anaerobic microorganisms, but these are described with huge variability
46 between each other. To cite some examples, Maddipati and coworkers (2011) purged 3 L of
47 culture medium (7.5 L total volume reactor) from oxygen using 12 L/h of N₂ for 24 hours.
48 Then, syngas was piped in the fermenter at 9 L/h (for a not-reported period) before
49 inoculation. Hoffmeister et al. (2016) purged 0.850 L of liquid culture medium (reactor of 2
50 L total volume), sparging N₂ for at least 12 h (in-flow gas rate was not reported). After this
51 step, feeding gas was provided at 30 L/h for 1 h. In Al Rowaihi and coworkers (2018) study,
52 a 1.6 L reactor was purged with 10 volumes of argon to remove any traces of oxygen from
53 the medium, followed by 10 purges with the feeding gas mixture. Other studies (Kantzow
54 and Weuster-Botz, 2016; Straub et al., 2014) describe a protocol in which 1 L of culture
55 medium, in a reactor of 2 L total volume, was sparged with the feeding gas mixture for at
56 least 12 h before inoculation of microorganism (in-flow gas rate was not reported). As
57 suggested from the abovementioned examples, this preliminary step for setting up an
58 anaerobic fermentation is time and resources consuming. Minimizing it would allow more
59 sustainable processes concerning the environmental and economic point of view and
60 optimize human efforts and employment of instruments. Nevertheless, some technical
61 constraints often arise in experimental and pilot plants regarding monitoring the dissolved
62 oxygen concentration and gaseous substrates saturation. Indeed, reactors could be designed
63 without probes for dissolved gases to reduce capital costs. Moreover, the development of
64 protocols might require dissolving gases different from those detected by the provided
65 probes.

66

Gas solubilization in a liquid phase is explained by the gas-liquid mass transfer laws, which describe the concentration gradient of a certain gas between phases. In Figure 1 the difference in concentration through the interphase is shown. There are three major stages of transfer between the gas bulk and the liquid bulk: the first one being the transfer of the gas from the bulk to the gas-liquid interphase, then the interphase itself, and finally from the liquid interphase to the liquid bulk (Doran, 1995).

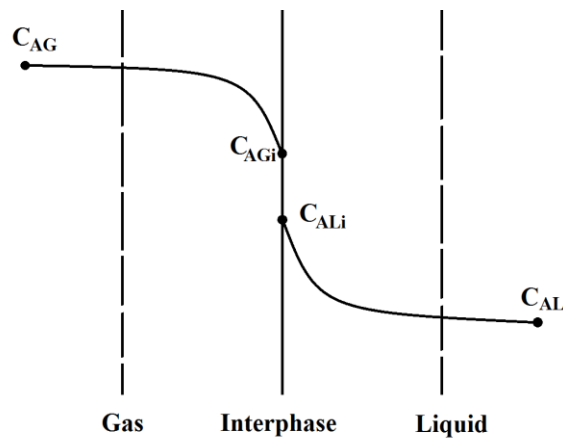


Figure 1. Diagram of the gas-liquid interface, with their respective concentrations. C_{AG} , concentration of the compound A in the gas phase bulk; C_{AL} , concentration of A in the liquid phase bulk; C_{AGi} and C_{ALi} , concentration of A in the gas and liquid interphase, respectively.

The liquid-phase mass transfer dominates the overall phenomena when working with gases with low solubility (like oxygen or hydrogen). The concentration at the liquid interphase can

82 be considered equal to the liquid concentration in equilibrium with the gas concentration in
83 the bulk.

84

$$N_A = k_L a \cdot (C_{AL}^* - C_{AL}) \quad (1)$$

85 where N_A is the rate of mass transfer of component A through the gas-liquid interphase, $k_L a$
86 is the combined mass-transfer coefficient, C_{AL}^* is the concentrations of A in the liquid phase
87 in equilibrium with C_{AG} , and C_{AL} is the actual concentration in the liquid phase. It can be
88 noticed that the driven force for the mass transfer is the difference between the equilibrium
89 and the current concentration. In some cases, these values can be directly measured. If it is
90 not possible, they can be smoothly calculated. Nevertheless, the mass-transfer coefficient is
91 not easy to estimate due to the nature of the fluids and the experimental conditions. The
92 composition of the liquid and gas phases, the stirring conditions, the geometry of the fluids
93 container, and many other factors affect this coefficient. Most authors have proposed models
94 with the following structure (Cooper et al., 1944; H Fukuda et al., 1968 (a); H. Fukuda et al.,
95 1968 (b); Richards, 1961; Van'T Riet, 1979)

96

$$k_L a = K \cdot \left(\frac{P}{V}\right)^\alpha \cdot (v_s)^\beta \cdot N^\gamma \quad (2)$$

97 where K , α , β and γ are constants that depend on the operating conditions as well as the
98 geometry of the reactor, while P/V , v_s and N are the volumetric power, the superficial gas
99 velocity, and frequency of the rotation of the mixer, respectively. As can be presumed, using
100 Equation 2 outside the boundaries of confidence will give inaccurate values. Besides, these
101 equations were proposed for oxygen transfer, which obligates the researcher to use the
102 diffusivity correlation between the gases and estimate the $k_L a$ of the scoped gas (Kery et al.,
103 2019). Another option for calculating the $k_L a$ is using dynamic methods (Munasinghe and

Khanal, 2010), which take much time and resources and also require an online measure of the dissolved gas, which sometimes, as described before, is not available.

This work presents a feasible method to estimate the time needed to remove a gaseous component from a liquid medium by replacing it with another gas (gas changing time). It is estimated using a classical and simplified liquid-gas phase equilibrium model. In particular, this work aims to describe a method that can be easily applied in the laboratory. It considers actual operational conditions and requires a few analytical instruments (i.e. gas analyzer) and informatics tools (i.e. an informatics program able to manage spreadsheets).

2. Materials and methods

2.1 Liquid phase composition

The liquid phase used in gas changing experiments was a culture medium for anaerobic bacteria. In 1 L of water, the medium contained K_2HPO_4 8.44 g; NaCl 2.9 g; yeast extract 2 g; KH_2PO_4 1.76 g; NH_4Cl 1 g; cysteine hydrochloride 0.5 g; $MgSO_4$ 0.180 g; resazurin 1 mg. Chemical reagents were purchased from Merck (DE).

2.2 Bioreactors

The reactor used for N_2 to CO_2 gas change and *vice versa* was a custom-adapted bioreactor manufactured by the H.E.L group (UK). The system consisted of a 2 L oil-jacketed vessel, 5 piston pumps for liquid injection (culture broth, base, acid, trace elements, and anti-foam), 4 Mass Flow Controller (MFC) for high in-flow gas rates (H_2 , CO_2 , N_2 , CO) (Vögtlin Instruments, CH) and 2 low in-flow gas rates MFCs (CO_2 and H_2) (Bronkhorst High-Tech BV, NL). Sparging of the gas was applied from the bottom of the vessel (via a micrometric

126 sparger). Stirring of the medium was mechanically maintained by one level of Ruston blades
127 connected to an impeller driven by a motor and baffles. An oil bath connected to the jacket
128 of the reactor allowed for sterilization (autoclaving of the vessel) and maintained the
129 operating temperature during experiments. The head plate of the reactor vessel was fitted
130 with pH, redox, liquid level, pressure, and temperature probes. A Back Pressure Regulation
131 (BPR) valve allowed pressure control at defined setpoints. The vessel was filled with 1L of
132 sterile medium during the gas changing experiments. The in-flow gas rate applied was 4.5
133 L/h, the stirring 400 rpm, and the reactor temperature 30°C.

134 The gas from the reactor outlet was released in a chemical hood or collected in sample bags
135 and analyzed by an off-line micro-GC. In experiments from N₂ to CO₂, the liquid medium
136 pumped in the reactor was previously sparged with 100% N₂ to remove oxygen. Gas out
137 sampling started immediately after the activation of the MFC for CO₂.

138 The reactor used for the gas change from air to N₂ and *vice versa* was a Biostat A reactor
139 (Sartorius Stedim Biotech, DE) consisting of a glass vessel of 1.5 L total volume, 4 peristaltic
140 pumps for liquid injection (culture broth, base, acid, and anti-foam), 2 MFCs (Air and N₂).
141 Stirring of the medium was mechanically provided by two levels of Rushton blades. The
142 reactor was sterilized by autoclaving. An electric heater placed around the outer side of the
143 glass vessel maintained a constant temperature during experiments. The head plate of the
144 reactor vessel was fitted with pH, foam, and temperature probes. During the gas changing
145 experiments, the vessel was filled with 0.5 L of sterile medium. The in-flow rate applied was
146 6 L/h, the stirring was 100 rpm, and the temperature was 30°C. The gas out from the reactor
147 was directly analyzed by a micro-GC. In the experiment from air to N₂, the liquid medium
148 was pumped into the reactor without oxygen purging. Gas out sampling started when MFC
149 for 100% N₂ was switched on.

2.3 Analytics and software

Gas composition for in-flowing and out-flowing gas was measured using an Agilent 490 Micro GC (Agilent, CA, USA) or a Micro GC Fusion (Inficon, CH). Agilent 490 Micro GC is equipped with the analytical columns Molsieve 5Å, using Argon as the carrier, and PoraPLOT U using Helium as the carrier. Micro GC Fusion is equipped with the analytical columns Molsieve 5Å and Rt-U-Bond, using Argon and Helium as carriers, respectively. Excel 2016 32-bit (Microsoft, USA) was used to analyze the experimental data to estimate the gas changing time.

2.4 Statistics

Two statistic indicators were calculated to evaluate how the predictive model and the real data correlated: the coefficient of determination (R^2) and the standard error of the estimate (σ_{est}), (Eq. (3) and (4) respectively). The statistical analysis was performed on the logarithmic results.

$$R^2 = 1 - \frac{\sum_{i=1}^n (y_i - y'_i)^2}{\sum_{i=1}^n (y_i - \bar{y})^2} \quad (3)$$

$$\sigma_{est} = \sqrt{\frac{\sum_{i=1}^n (y_i - y'_i)^2}{n}} \quad (4)$$

where:

y_i : is an actual experimental value.

y'_i : is the predicted value.

n : is the number of experimental data.

\bar{y} : is the mean value of the experimental data.

Formatted: Not Highlight

Formatted: Not Highlight

Formatted: Not Highlight

Formatted: Not Highlight

Formatted: Not Highlight

Formatted: Not Highlight

Formatted: Not Highlight

Formatted: Not Highlight

Formatted: Not Highlight

Formatted: Not Highlight

Formatted: Not Highlight

Formatted: Not Highlight

Formatted: Not Highlight

Formatted: Not Highlight

Formatted: Not Highlight

Formatted: Not Highlight

Formatted: Not Highlight

Formatted: Not Highlight

Formatted: Not Highlight

3. Results

3.1 Model

The model formulated was based on the following system (Figure 2). A certain gas (i) is bubbled at a rate of $G_{in} \cdot y_{i,in}$ in a reactor with V_L volume of liquid and V_G volume of gas in the headspace. The temperature (T) and the pressure (P) is fixed. The gas outlet (G_{out}) has a fraction of the i gas ($y_{i,out}$). Inside the liquid phase, there is a certain concentration of dissolved gas ($C_{i,L}$).

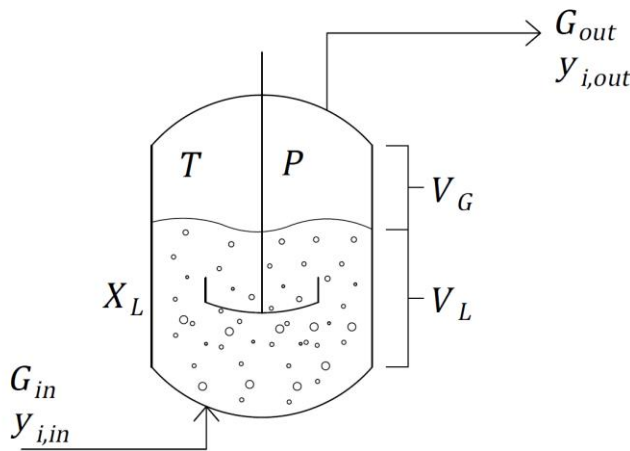


Figure 2. The system considered in the model.

Where:

G: Molar Flow (mmol/min).

y: Molar fraction in the gas.

184 V: Volume (m³).

185 C: Concentration (mmol/m³).

186 T: Temperature (K).

187 P: Pressure (Pa).

188 Subscript:

189 L: in/of the liquid.

190 G: in/of the gas.

191 in: Inlet.

192 out: Outlet.

193 *i*: from compound *i*.

194 Three mass balances can be proposed for this system: the global balance of compound *i* (Eq.
195 5), the balance of compound *i* in the liquid phase (Eq. 6), and the balance of compound *i* in
196 the gas phase (Eq. 7) which assumes the gas as an ideal one.

$$\frac{dn_i}{dt} = G_{in} \cdot y_{i,in} - G_{out} \cdot y_{i,out} \quad (5)$$

$$\frac{dn_{i,L}}{dt} = k_L a \cdot V_L \cdot (C_{i,L}^* - C_{i,L}) \quad (6)$$

$$\frac{dn_{i,G}}{dt} = \frac{V_G}{R \cdot T} \cdot \frac{dp_i}{dt} \quad (7)$$

197 where n_i are the moles of the *i* compound, p_i is the partial pressure of *i* in the headspace, and

198 $C_{i,L}^*$ is the equilibrium concentration of *i* in the liquid.

199 The global accumulation of moles in the system will be equal to the sum of the accumulation
200 in both gas and liquid phases (Eq. 8).

201

$$\frac{dn_i}{dt} = \frac{dn_{i,L}}{dt} + \frac{dn_{i,G}}{dt} \quad (8)$$

202

203 This allows the generation of a new equation (Eq. 9) by replacing Eq (5), (6), and (7) in (8).

$$\frac{V_G}{R \cdot T} \cdot \frac{dp_i}{dt} = G_{in} \cdot y_{i,in} - G_{out} \cdot y_{i,out} - k_L a \cdot V_L \cdot (C_{i,L}^* - C_{i,L}) \quad (9)$$

204 On the other hand, from Eq (6), it is possible to obtain a relation between time and $C_{i,L}$

205 (assuming $C_{i,L}^*$ constant during short periods).

$$V_L \cdot \frac{dC_{i,L}}{k_L a \cdot V_L \cdot (C_{i,L}^* - C_{i,L})} = dt \quad (10)$$

$$\int \frac{dC_{i,L}}{k_L a \cdot (C_{i,L}^* - C_{i,L})} = \int dt \quad (11)$$

$$\frac{-1}{k_L a} \cdot (\ln(C_{i,L}^* - C_{i,L}) - \ln K) = t \quad (12)$$

$$\ln \frac{(C_{i,L}^* - C_{i,L})}{K} = -t \cdot k_L a \quad (13)$$

$$\frac{(C_{i,L}^* - C_{i,L})}{K} = e^{-t \cdot k_L a} \quad (14)$$

$$C_{i,L} = C_{i,L}^* - K \cdot e^{-t \cdot k_L a} \quad (15)$$

206 where K is the constant of integration. By replacing Eq. (15) into Eq. (9) the following

207 expression is obtained

$$\frac{V_G}{R \cdot T} \cdot \frac{dp_i}{dt} = G_{in} \cdot y_{i,in} - G_{out} \cdot y_{i,out} - k_L a \cdot V_L \cdot (C_{i,L}^* - C_{i,L} + K \cdot e^{-t \cdot k_L a}) \quad (16)$$

208 If no i compound is injected into the system ($y_{i,in} = 0$), Eq. (16) could be expressed as

$$\frac{V_G}{R \cdot T} \cdot \frac{dp_i}{dt} + G_{out} \cdot y_{i,out} = -k_L a \cdot V_L \cdot K \cdot e^{-t \cdot k_L a} \quad (17)$$

209 Since the partial pressure of the i compound (p_i) in the headspace will be equal to the total
210 pressure (P) times the molar fraction in the outlet stream, Eq. (17) becomes:

$$\frac{V_G}{R \cdot T} \cdot \frac{d(P \cdot y_{i,out})}{dt} + G_{out} \cdot y_{i,out} = -k_L a \cdot V_L \cdot K \cdot e^{-t \cdot k_L a} \quad (18)$$

211 Assuming a constant pressure during the whole process, Eq. (18) can be rewritten as

$$\frac{V_G \cdot P}{R \cdot T} \cdot \frac{dy_{i,out}}{dt} + G_{out} \cdot y_{i,out} = -k_L a \cdot V_L \cdot K \cdot e^{-t \cdot k_L a} \quad (19)$$

212 Besides, we can assume that:

$$\frac{V_G \cdot P}{R \cdot T} = n_G \quad (20)$$

$$n_G \cdot \frac{dy_{i,out}}{dt} + G_{out} \cdot y_{i,out} + k_L a \cdot V_L \cdot K \cdot e^{-t \cdot k_L a} = 0 \quad (21)$$

213 where n_G is the total amount of gas moles in the system. By solving the differential equation,
 214 Eq. (22) is obtained:

$$y_{i,out} = K_1 \cdot e^{-t \frac{G_{out}}{n_G}} + \frac{k_L a \cdot V_L \cdot K \cdot e^{-t \cdot k_L a}}{k_L a \cdot n_G - G_{out}} \quad (22)$$

215 where K_1 is a new constant that comes from the solution of the differential equation. In Eq.
 216 (22), it can be noticed that if $G_{out} \ll k_L a \cdot n_G$ then

$$y_{i,out} \approx K_1 \cdot e^{-t \frac{G_{out}}{n_G}} + \frac{V_L \cdot K}{n_G} \cdot e^{-t \cdot k_L a} \quad (23)$$

217 Since the value of the first exponent will be greater than the second and if the constants have
 218 the same order of magnitude, the first term will dominate the value of $y_{i,out}$.

$$y_{i,out} \approx K_1 \cdot e^{-t \frac{G_{out}}{n_G}} \quad (24)$$

219 On the other side, if $G_{out} \gg k_L a \cdot n_G$ then

$$y_{i,out} \approx K_1 \cdot e^{-t \frac{G_{out}}{n_G}} - \frac{k_L a \cdot V_L \cdot K}{G_{out}} \cdot e^{-t \cdot k_L a} \quad (25)$$

220 At the beginning of the gas change process, the value of $\frac{k_L a \cdot V_L \cdot K}{G_{out}}$ in Eq. (25) makes the second
221 term have a small influence on the value of $y_{i,out}$. As time passes, the rate of decrease is
222 greater. Nevertheless, since $y_{i,out}$ cannot take negative values, the value of the second term
223 cannot be greater than the first one. Hence, for small values of time:

$$y_{i,out} \approx K_1 \cdot e^{-t \frac{G_{out}}{n_G}} \quad (26)$$

224 It can be noticed that the two variables that can be controlled by changing the stirring speed
225 or the gas flow ($k_L a$ and G_{out}) can dominate the process. When the molar flow dominates
226 the process ($G_{out} \gg k_L a \cdot n_G$), the phenomenon occurs faster rather than when the
227 volumetric gas transfer coefficient ($G_{out} \ll k_L a \cdot n_G$) dominates the process. Besides, since
228 $k_L a$ depends on the volumetric power that is controlled by the stirring rate and the flow, the
229 relation between G_{out} and $k_L a$ can be described as a relation between G and the stirring
230 velocity of the reactor. This could be researched in future work.

231 This simplified exponential model will describe the decay of the concentration of a
232 purged gas and it can be applied to predict the gas exchange time of a determined
233 system if the constant parameters are available. Using a semilogarithmic graph the
234 slope will represent the value of $\frac{G_{out}}{n_G}$ and the intercept the logarithm of K_1 . The following
235 section describes the protocol to obtain the gas change time.

236 3.2. Protocol

237 To estimate the gas changing time the following steps need to be executed:

- 1) Take a sample of the outlet flow of gas from the reactor at the beginning of the gas changing process and measure its molar composition in percentage or fraction through a gas analyzer.
- 2) Repeat the same process regularly with an interval of time determined by the researcher. An interval of 5 minutes is recommended .
- 3) The sampling can stop after the fraction of the purged gas reaches half of its value at the beginning of the gas changing process.
- 4) On a spreadsheet, create a graph with the time values on the X-axis and the natural logarithm of the fraction or percentage of the purged gas on the Y-axis.
- 5) Obtain the linear regression of the data.
- 6) Obtain the equation of the linear regression line and the R-squared value.
- 7) The R-squared value needs to be higher than 0.99.
- 8) Graphically obtain the value of time that will fulfill the desired gas change. The linear regression intercept will be approximately $\ln(K_1)$ and the slope $-\frac{G_{out}}{n_G}$ of Eq. (22).

3.3. Model validation

Figures 3-6 report the decrease of the gas purged from the reactor throughout the gas changing experiments. Figures 3 and 4 show data from N₂ to CO₂ and from CO₂ to N₂, respectively. Similarly, Figures 5 and 6 describe experiments using air and N₂. According to the analysis of the in-let gas, air sparged in the reactor had 20.9 % of O₂ and 79.05% of N₂. The purge of air using pure nitrogen and *vice-versa* was evaluated by monitoring the variation of the oxygen molar fraction in the out-gas.

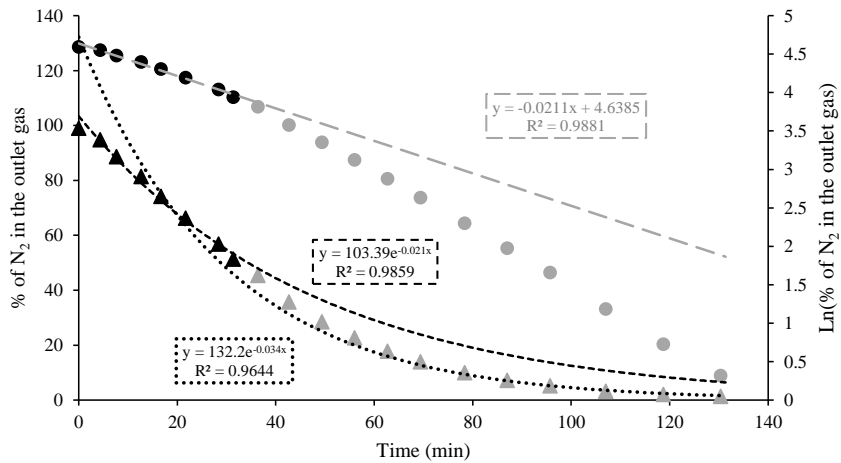


Figure 3: Purging of nitrogen using carbon dioxide. Triangles: experimental values; Dots: natural logarithm of the experimental data; Dotted black line: exponential curve generated by all the experimental data; Dashed black line: exponential curve obtained by using black triangles; Dashed gray line: linear curve obtained by considering the black dots.

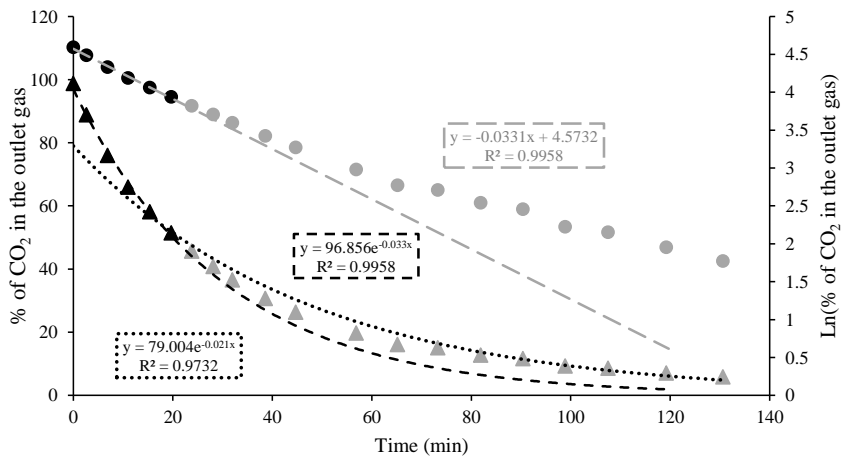


Figure 4: Purging of carbon dioxide using nitrogen. Triangles: experimental values; Dots: natural logarithm of the experimental data; Dotted black line: exponential curve generated by all the experimental data; Dashed black line: exponential curve obtained by using black triangles; Dashed gray line: linear curve obtained by considering the black dots.

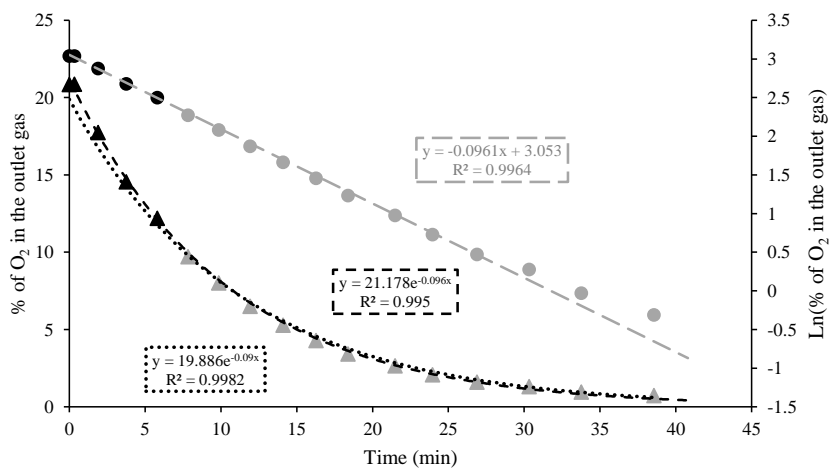


Figure 5: Purging of air using nitrogen. Triangles: experimental values; Dots: natural logarithm of the experimental data; Dotted black line: exponential curve generated by all the experimental data; Dashed black line: exponential curve obtained by using black triangles; Dashed gray line: linear curve obtained by considering the black dots.

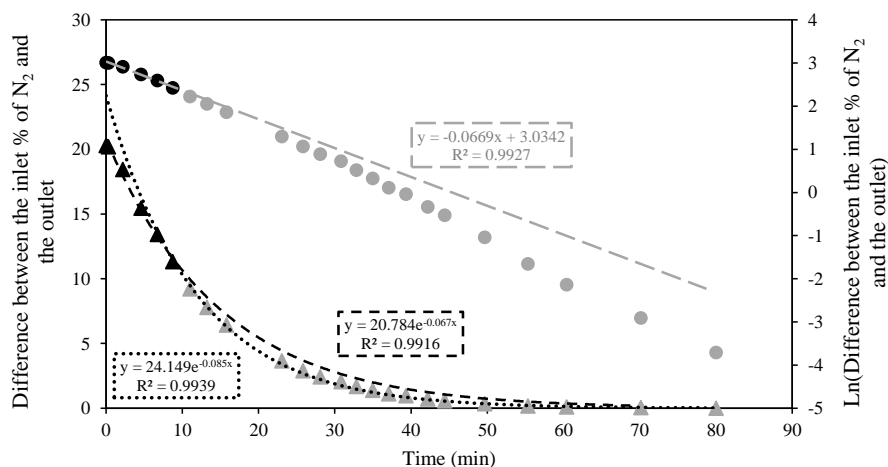


Figure 6: Purging of nitrogen using air. Triangles: experimental values; Dots: natural logarithm of the experimental data; Dotted black line: exponential curve generated by all the experimental data; Dashed black line: exponential curve obtained by using black triangles; Dashed gray line: linear curve obtained by considering the black dots.

Experimental data were plotted and the model was applied. The correlation between data and the model was evaluated. It can be seen that data from each experiment fit an exponential curve (dotted black lines in Figures 3-6). Following the protocol, the linear correlation between the natural logarithm of the out-gas composition and the time was obtained for each purged gas (black dots and dashed gray line in Figures 3-6). It can be seen that in experiments involving carbon dioxide the predicting lines did not correlate accurately with the experimental data, whereas in the experiments with air and nitrogen the predictive models fit the experimental data with greater precision. Table 1 reports the statistics calculated for each gas changing experiment.

Table 1: Statistical analysis between the predictive model and the experimental data.

Formatted: Not Highlight

Experiment	N ₂ to CO ₂	CO ₂ to N ₂	Air to N ₂	N ₂ to air
n	20	15	17	24
$\sum_{i=1}^n (y_i - y'_i)^2$	8.57	7.98	0.17	7.82
$\sum_{i=1}^n (y_i - \bar{y})^2$	34.24	15.06	19.12	84.88
R^2	0.7496	0.47	0.9909	0.9079
σ_{est}	0.6547	0.6318	0.101	0.5707

Formatted: Not Highlight

Formatted: Not Highlight

Formatted: Not Highlight

Formatted: Not Highlight

Formatted: Not Highlight

Formatted: Not Highlight

Formatted: Not Highlight

Formatted: Not Highlight

Formatted: Not Highlight

Formatted: Not Highlight

The value of the X-axis made it possible to extract the time that fulfills the desired gas change. For example, in the experimental condition applied, complete purging of oxygen using nitrogen required around 40 minutes (Figure 5). The maximum difference between the modeled values and experimental data was 0.4%. For the experiments involving CO₂, a different reactor was used and other experimental conditions were applied. Therefore, a different gas changing time was needed. Figure 3 shows that the time required to completely change the gas from nitrogen to carbon dioxide was around 200 minutes. The error between the model and the experimental data was more variable. In fact, when the gas change was completed, the error was 1.9 % of the gas composition. In the central part of the curve, at around 70 minutes, the maximum error was of 9.9 %.

4. Discussion

The protocol proposed describes an easily applicable method to estimate the gas changing time in the laboratory routine. It aims to consume little time and resources, considering actual operating conditions, and requires few analytic instruments and informatics tools.

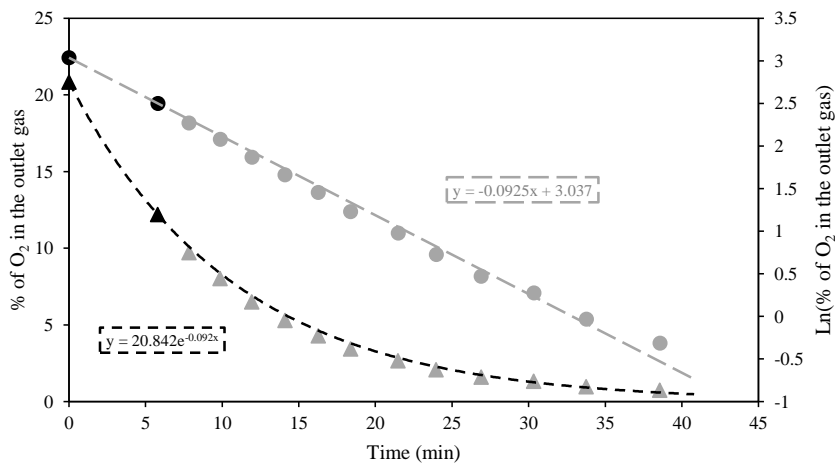
In all the experiments, the error between the actual values and the values predicted by the model was less than 10% of the gas composition. The biggest difference recorded was in

experiments involving CO₂. In experiments that did not involve carbon dioxide, the maximum error was reduced to less than 0.8%. The bigger error found with CO₂ could be explained by the chemical equilibrium that carbon dioxide has in aqueous solutions, which is not considered in the proposed model. In fact, carbon dioxide reacts with water and produces carbonic acid. This reaction has slow kinetics (for more details see Stumm and Morgan, 1995) and creates a stock of CO₂ in the liquid phase, which moves towards equilibrium with the gas phase. It can explain why the predictive model showed a faster decrease in the CO₂ fraction than the measured values (Figure 4). Another factor that could have affected results with CO₂ was the variable pressure inside the reactor during the gas change. In the experiments that involved this gas, the pressure fluctuated between 1.51 bar and 1.76 bar. In particular, the reactor pressure was set at 1.76 bar, with a constant in-flow gas rate and opening of the valve for pressure regulation. After starting the sparging of the medium with CO₂, the pressure quickly decreased to 1.51 bar. It then returned to the initial value (1.76 bar) when the gas change was completed. The assumption of a constant pressure done during the deduction of the model might explain the discrepancy between the experimental data and the model.

According to the statistical analysis, the air to N₂ model best correlated to the experimental data, followed by the N₂ to air change. When the gas change was from nitrogen to carbon dioxide, the coefficient of determination was higher than when it was from carbon dioxide to nitrogen. Considering the value of the standard error of the estimate, the accuracy of the gas change from carbon dioxide to nitrogen is slightly more accurate than the reverse process experiment. Nevertheless, in both cases, the statistical analysis suggested a worse accuracy of the model in experiments involving CO₂ than in experiments involving air, probably due to the effect of the chemical equilibrium of carbon dioxide in water.

Formatted: Not Highlight

332 The model is for researchers looking for an affordable and practical method to improve their
 333 experiments' efficiency. The specific experimental conditions and the constraints related to
 334 the availability of analytical instruments can make the time between each measurement very
 335 variable. This work found out that, purging oxygen, the model could fit very well with the
 336 experimental data measuring only two samples, one at the beginning and another when the
 337 gas was half of its initial concentration (Figure 7).



338

339 Figure 7: Purging of air using nitrogen. Triangles: experimental values; Dots: natural
 340 logarithm of the experimental data; Dashed black line: exponential curve obtained by using
 341 only black triangles; Dashed gray line: linear curve obtained by considering the black dots.

342 It is important to remember that the time required for gas change inside the reactor will vary
 343 with the conditions of stirring, temperature, pressure, gas in-flow rate, gas and media
 344 compositions. If the conditions do not change, the time predicted in one experiment can be

used in the following experiments. If one or more factors change, it is recommended to re-evaluate the gas changing time using this protocol.

5. Conclusion

The proposed protocol allows researchers to predict the time required to completely exchange the gas in a reactor containing liquid media, and it takes into account the actual experimental condition applied in a specific run. Purging of an unwanted gas from the reactor often is based on bibliographic data. These calculations, in many cases, are not accurate enough for a specific situation because of the differences in both reactor and experimental settings (reactor design, working volume of liquid and gas phases, in-flow rate of a specific gas, stirring equipment and speed). The described protocol can be easily implemented in the laboratory. Hence, it seeks to be simple for sampling procedure, calculation, and requirements in terms of human and time efforts, equipment, and software.

The model's correlation and accuracy were high when air was purged with nitrogen, which is often the first step in setting up an anaerobic fermentation. For cases involving CO₂, the correlation and the accuracy were lower. To improve the model, specific CO₂ modeling should include the chemical equilibrium of this gas in water. Moreover, a comparison between the k_{La} -dominant process and the molar flow-dominant process should also be performed for further model validation. Nevertheless, the proposed methodology for calculating the gas changing time will contribute to the efficient use of resources and time during experiments involving other gases, mainly oxygen, which is a pivotal step for many processes involving anaerobic reactions.

Formatted: Not Highlight

Acknowledgments

We would like to thank Prof. Germán Eduardo Aroca Arcaya, Prof. Raúl Conejeros (Pontificia Universidad Católica de Valparaíso, Valparaíso, Chile) and Giuseppe Pietricola, Ph.D. (Politecnico di Torino, Torino, Italy) for advices and revisions that improved the manuscript. Moreover, we would like to thank Prof. Carminna Ottone (Pontificia Universidad Católica de Valparaíso, Valparaíso, Chile) for supporting the mobility between the research institutions allowing this collaboration.

Fundings

This research did not receive any specific grant from funding agencies in the public, commercial, or not-for-profit sectors.

References

- Al Rowaihi, I.S., Kick, B., Grötzinger, S.W., Burger, C., Karan, R., Weuster-Botz, D., Eppinger, J., Arold, S.T., 2018. A two-stage biological gas to liquid transfer process to convert carbon dioxide into bioplastic. *Bioresour. Technol. Reports* 1, 61–68. <https://doi.org/10.1016/j.biteb.2018.02.007>
- Chauvy, R., Meunier, N., Thomas, D., De Weireld, G., 2019. Selecting emerging CO₂ utilization products for short- to mid-term deployment. *Appl. Energy* 236, 662–680. <https://doi.org/10.1016/j.apenergy.2018.11.096>
- Cooper, C.M., Fernstrom, G.A., Miller, S.A., 1944. Performance of Agitated Gas-Liquid Contactors—Correction, *Industrial and Engineering Chemistry. UTC*.

389 <https://doi.org/10.1021/ie50417a601>

390 Doran, P.M., 1995. *Bioprocess Engineering Principles*. Academic press.

391 Fukuda, H., Sumino, Y., Kansaki, T., 1968. Modified equations for volumetric oxygen
392 transfer coefficient. *J. Ferment. Technol.* 46, 829–837.

393 Fukuda, H., Sumino, Y., Kansaki, T., 1968. Scale-Up of Fermenters. II. Modified Equations
394 for Power Requirement. *J. Ferment. Technol.* 46, 838.

395 Hoffmeister, S., Gerdorf, M., Bengelsdorf, F.R., Linder, S., Flüchter, S., Öztürk, H., Blümke,
396 W., May, A., Fischer, R.J., Bahl, H., Dürre, P., 2016. Acetone production with
397 metabolically engineered strains of *Acetobacterium woodii*. *Metab. Eng.* 36, 37–47.
398 <https://doi.org/10.1016/j.ymben.2016.03.001>

399 Kantzow, C., Weuster-Botz, D., 2016. Effects of hydrogen partial pressure on autotrophic
400 growth and product formation of *Acetobacterium woodii*. *Bioprocess Biosyst. Eng.* 39,
401 1325–1330. <https://doi.org/10.1007/s00449-016-1600-2>

402 Kery, K., Kresnowati, P., Setiadi, T., 2019. Evaluation of gas mass transfer in reactor for
403 syngas fermentation. *AIP Conf. Proc.* 2085. <https://doi.org/10.1063/1.5094986>

404 Maddipati, P., Atiyeh, H.K., Bellmer, D.D., Huhnke, R.L., 2011. Ethanol production from
405 syngas by *Clostridium* strain P11 using corn steep liquor as a nutrient replacement to
406 yeast extract. *Bioresour. Technol.* 102, 6494–6501.
407 <https://doi.org/10.1016/j.biortech.2011.03.047>

408 Munasinghe, P.C., Khanal, S.K., 2010. Syngas fermentation to biofuel: Evaluation of carbon
409 monoxide mass transfer coefficient (kLa) in different reactor configurations. *Biocatal.*
410 *Bioreact. Des.* 26, 1616–1621. <https://doi.org/10.1002/btpr.473>

411 Richards, J.W., 1961. Studies in aeration and agitation. *Prog Ind Microbiol* 3, 141–172.

412 Saravanan, A., Senthil kumar, P., Vo, D.V.N., Jeevanantham, S., Bhuvaneswari, V., Anantha

413 Narayanan, V., Yaashikaa, P.R., Swetha, S., Reshma, B., 2021. A comprehensive
414 review on different approaches for CO₂ utilization and conversion pathways. Chem.
415 Eng. Sci. 236, 116515. <https://doi.org/10.1016/j.ces.2021.116515>

416 Shi, J., Jiang, Y., Jiang, Z., Wang, Xueyan, Wang, Xiaoli, Zhang, S., Han, P., Yang, C., 2015.
417 Enzymatic conversion of carbon dioxide. Chem. Soc. Rev. 44, 5981–6000.
418 <https://doi.org/10.1039/c5cs00182j>

419 Straub, M., Demler, M., Weuster-Botz, D., Dürre, P., 2014. Selective enhancement of
420 autotrophic acetate production with genetically modified *Acetobacterium woodii*. J.
421 Biotechnol. 178, 67–72. <https://doi.org/10.1016/j.jbiotec.2014.03.005>

422 Stumm, W., Morgan, J.J., 1995. Aquatic chemistry : Chemical equilibria and rates in natural
423 waters, John Wiley & Sons. <https://doi.org/10.1094/asbcmoa-beer-13>

424 Van'T Riet, K., 1979. Review of Measuring Methods and Results in Nonviscous Gas-Liquid
425 Mass Transfer in Stirred Vessels. Ind. Eng. Chem. Process Des. Dev. 18, 357–364.
426 <https://doi.org/10.1021/i260071a001>